Measuring the Specific Heat Capacity of Thermal Insulation Materials Used in Buildings by Means of a Guarded Hot Plate Apparatus

Karim Ghazi Wakili[1] · Wolfgang Rädle[1] · Thomas Rohner[1]

Abstract

The specific heat capacity of building insulation materials is rather difficult to be determined using the conventional calorimetric methods. This is due to the small samples required for these methods which are not representative of the insulation material. Larger samples would not fulfill the requirements of the lumped system. Methods based on the transient heat transfer using heating wires or planes are commonly quick but less accurate measurements as they only consider the volume near the surface of the sample and need additional corrections and calibrations. The present investigation is based on a transient temperature control procedure using a common guarded hot plate device, which is normally used to determine the thermal conductivity of insulation materials. The procedure was performed on two different materials: one wood-based (wood fiber) and one mineral-based (expanded perlite). The results show a value of about 1200 J·kg^{-1}·K^{-1} for the former and 600 J·Kg^{-1}·K^{-1} for the latter. This method can also be extended to other thermal insulation materials for building application.

Keywords Expanded perlite · Guarded hot plate · Insulation materials · Specific heat · Transient heat transfer · Wood fiber

1 Introduction

The usual calorimetric method to determine the specific heat capacity of materials is based on the simple principle of immersing a sample of the material which has been in thermal equilibrium of an environment of temperature T_s into a calorimeter with a certain amount of water kept at a temperature of T_w. Based on the resulting equilibrium temperature T_e together and the sample mass, the specific heat

✉ Karim Ghazi Wakili
karim.ghaziwakili@bfh.ch

[1] Structures and Architecture, Bern University of Applied Sciences Institute for Timber Construction, Solothurnstrasse 102, CH-2500 Biel 6, Switzerland

capacity of the latter can be calculated. This rather straight forward method is perfect for homogeneous and dense materials with medium to good thermal conductivity (> 0.2 W·(m·K)$^{-1}$) [1]. The matter differs for insulation materials of low density (< 200 kg·m^{-3}) and low thermal conductivity (< 0.05 W·(m·K)$^{-1}$). First, the size of the sample for low density materials must be chosen larger to get enough mass and hence enough thermal energy to be detectable by the measuring device. Another point is the matter how representative a small sample is due to inhomogeneity in the insulation materials itself. The third point is the assumption that the temperature distribution within the sample is considered uniform *i.e.,* the so-called "lumped system analysis" is considered applicable [2]. The criteria for this are linked to the "characteristic length" of the sample (1) to be immersed in the water and the "Biot number" (2):

$$L_s = V/A \tag{1}$$

where V is the volume (m^3), and A is the surface (m^2) of the sample and

$$Bi = \left(h \bullet L_s \right) / \lambda_s \tag{2}$$

where h is the heat transfer coefficient for convection between the surface of the sample and the water (well stirred to reach a homogeneous temperature) and λ_s the thermal conductivity of the sample.

The assumption for a uniform temperature distribution within the sample is applicable only if

$$Bi < 0.1 \tag{3}$$

Considering a sample of $5 \times 5 \times 5$ cm^3 size, a thermal conductivity of 0.04 W·(m·K)$^{-1}$, and a typical convective heat transfer between water and sample of 100 W·m^{-2}·K^{-1} [2] a Biot number of over 25 will result. Even with a wooden sample with a thermal conductivity of 0.15 W·mK^{-1} the corresponding Biot number will be larger than 5. In both cases, the criterion for the "lumped system" will not be fulfilled. Any smaller sample size which would reduce the Biot number would not be representative of the insulation material under investigation.

There are several other methods to determine the specific heat capacity of insulating materials. They are all based on the transient heat transfer dominated by the thermal diffusivity a (m^2·s^{-1}). This parameter depends in turn on the three major properties of the material namely the thermal conductivity λ, the density ρ, and the specific heat capacity c:

$$a = \lambda / (\rho \bullet c) \tag{4}$$

In order to get the value of the specific heat capacity of a material by using the transient methods, its density and thermal conductivity have to be known or approximated by some calibration measures.

Mann *et al.* [3] determined specific heat thermal conductivity for glass and other semi-transparent materials from dynamic temperature data in the early 1990's. This was done by using a unique technique to obtain high-quality dynamic temperature

data from glass test plates using thermocouples fused to the glass, a method not applicable to building insulation materials. Another more adequate method was reported by Bouguerra [4] using a transient plane source technique. This method detects a temperature increase due to electrical heating of a pair of samples and makes use of an electrical resistance circuit to measure the dissipated heat. It results in a rather local value of the thermal diffusivity and makes use of numerical approximations in its analysis.

Boumaza and Redgrove used the transient plane source technique for the determination of thermal conductivity of extruded polystyrene [5] but did not report about the specific heat capacity although they measured the value of the thermal diffusivity of the insulation samples. Ohmura *et al.* determined the specific heat of a standard mineral wool specimen at temperatures between 100 °C and 1000 °C by means of a specially developed apparatus based on the drop calorimeter method which is also a transient method [6]. They assume homogeneous temperature distribution in the sample and reach an accuracy of ± 10 % with respect to the declared standard value. Using the measured transient temperature response, Zhao *et al.* used a special numerical method to identify the equivalent radiative properties and thermal conductivities of fibrous insulations [7]. The corresponding specific heat was not determined but taken from a previous publication. Park *et al.* suggested a lumped parameter circuit representing a building thermal model using thermal-electric analogy [8, 9]. They identified the circuit components the thermal resistor and the thermal capacitor from the heat balance equation and experimental results. The method is applicable to whole buildings but not to single materials. Luo *et al.* made use of a finite volume scheme and Fourier analysis to calculate the thermal capacitance (defined as the product of density and specific capacity) and thermal conductivity for a building construction layer from monitored inner/outer surface temperatures and heat fluxes [10]. This is an elaborate procedure and needs in situ measurements on the construction itself and less adequate for testing insulation materials as such.

Barreneche *et al.* reported on a device developed at the University of Lleida [11] to determine the specific heat capacity of gypsum blocks at lab scale. This was mainly designed for characterizing Phase Change Materials (PCM) added to the gypsum. Czajkowski *et al.* reported that high accuracy required for the specific heat measurements of wood-based materials was achieved only for experiments with high-mass samples, in contrast to traditional Differential Scanning Calorimetry (DSC) measurements with smaller samples usually less than 100 mg [12]. They estimated a minimum sample size of 0.7 dm^3 and designed a special calorimeter for their purpose. Barreca *et al.* used also infrared thermography and heat flow meters to evaluate the overall capacity of whole building components using on-site measurements [13]. An elaborate review dealing with several methods of calculating the heat capacities of materials, with the aim of providing an overview of the thermal behavior of lightweight insulation materials has been made by Ricciu *et al.* [14]. The authors proposed a simple method able to evaluate the specific heat capacity of real scale building materials with high porosity, low thermal conductivity, and low density. They used the transient method, in which a heat flow meter apparatus was used in a climatic chamber to measure the thermal conductivity of the tested material to determine its specific heat capacity. Lakatos *et al.* reported on thermal

conductivity and specific heat capacity measurements executed in a Netzsch 446 small equipment. According to them, this apparatus measures specific heat capacity by heating the sample on a step-by-step basis, while the two plates are maintained precisely at the same temperature [15]. No further elaboration of the measurement details has been supplied. It seems clear that the method was based on measuring a transient heat distribution.

A previous publication of one of the present authors [16] reported on the deployment of a heat flow meter apparatus with two identical insulation material samples to determine their specific heat capacity making use of a numerical identification method and a thermal distribution simulation to analyze the measured thermal response to the imposed heat steps. The present investigation is based on a transient temperature control procedure and makes use of a common guarded hot plate (GHP) which is much better controlled than a heat flow meter apparatus and has the higher precision in adjusting and maintaining temperature levels on its hot and cold plates. Additionally, the whole apparatus is kept in a fully insulated box to minimize the influence of the air temperature of the lab.

2 Materials

There are many thermal insulations for buildings on the market based on different primary materials. Two different types of materials were chosen to perform on them in the present investigation. One of them is a wood-based material generally known to have a higher specific heat capacity than mineral-based or polymer-based insulation materials, and the other is a perlite insulation *i.e.,* mineral-based (Fig. 1). For the measurements in the GHP, two samples of each material were cut and put together to have an overall size of 900 mm × 900 mm. Some of their properties are summarized in Table 1. The values for the thermal conductivity at 20 °C for all samples have been determined previously by means of the GHP apparatus according to the respective European CEN Standard [17].

As the following measurements are basically in the transient state, moisture transport and redistribution can also take place. To get an approximative value for this, it

Fig. 1 Samples of wood fiber and expanded perlite insulation materials

**Table 1** Summary of the material properties of the investigated samples

Material	Density [kg·m^{-3}]	Therm. Conductivity [W·(m·K)$^{-1}$]	Thickness [mm]	Length & width [mm]
Wood fiber	104 ± 4	0.038 ± 0.002	60.3 ± 0.1	800 × 800
Expanded perlite	96 ± 4	0.045 ± 0.002	59.0 ± 0.1	900 × 900

is necessary to know the sorption isotherms of the investigated materials. This has been done using 4 samples of 100 mm × 100 mm of each material and conditioning them in a climate chamber at different levels of relative humidity. Figure 2 shows the respective sorption isotherms of the wood fiber and the expanded perlite.

At a relative humidity of 50 % of the air in the lab, the amount of moisture uptake is low for the wood fiber and relatively modest for expanded perlite. Knowing that diffusive moisture transport is much slower than heat transfer at temperature gradients of 10 K, the redistribution of moisture will not have a detectable influence on the results. This is since the samples for the GHP measurements have been conditioned at 23 °C and 50 % rh previously and the whole lab is kept at this climate.

3 Measurements

The measurements were carried out in a guarded hot plate apparatus (Netzsch Taurus Instruments) which is installed in a box and can measure thermal conductivity of materials and composites in both vertical and horizontal position. For our purpose, the single plate horizontal configuration had been chosen. A schematic representation of the two sample halves is shown in Fig. 3. The dotted line at the center shows the metering area within which the heat flow lines are kept unidirectional (no lateral heat flow). In this configuration, a compensation heating element (white in Fig. 3) is
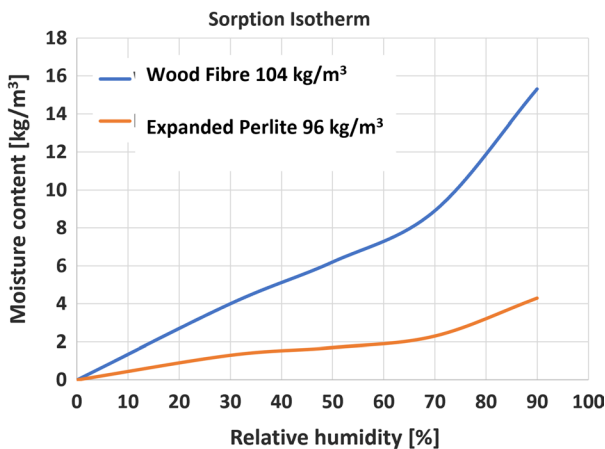
Fig. 2 Sorption isotherms at 23 °C for the investigated wood fiber and expanded perlite boards

Outer box (black line)
Insulation around (yellow)
Upper cooling plate (blue)
Compensation heating element (White)
Heating plate (red), 5 Thermocouples
First sample half
5 Thermocouples between halves
Second sample half
Lower cooling plate (blue), 5 Thermocouples
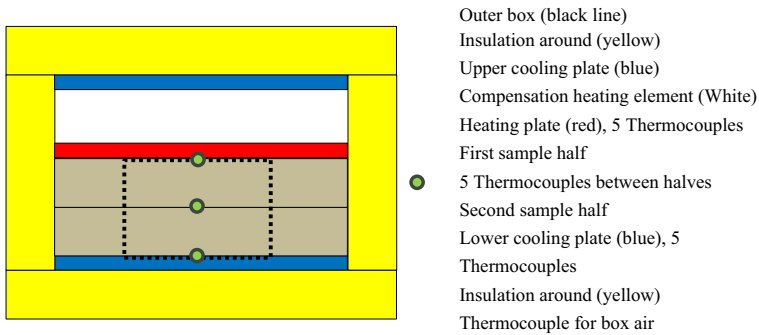Insulation around (yellow)
Thermocouple for box air

Fig. 3 The schematic representation of the guarded hot plate (GHP) apparatus with samples and 15 additional thermocouples represented by 3 dots. For the present investigation, the single plate horizontal configuration *i.e.,* a heating plate on top and a cooling plate at the bottom was used. The dotted rectangle indicates the metering area (drawing not to scale)

installed between the heating plate (red in Fig. 3) and the upper cooling plate. The temperature difference between the compensation heating plate and the heating plate is kept below 0.01 K so that no heat flows upwards but only downwards through the two sample halves. Figure 4 shows one of the sample halves of the wood fiber insulation together with the additionally installed thermocouples (type K) represented by the round dot at the center of Fig. 3. The thermocouples for standard tests (type K) are not shown.

The first step of the measuring procedure was to build up a constant temperature gradient between the warm and the cold plate and reach a steady state. This status has been monitored by the additional thermocouples placed on the warm and the cold side as well as between the two sample halves. At a certain point of time, the
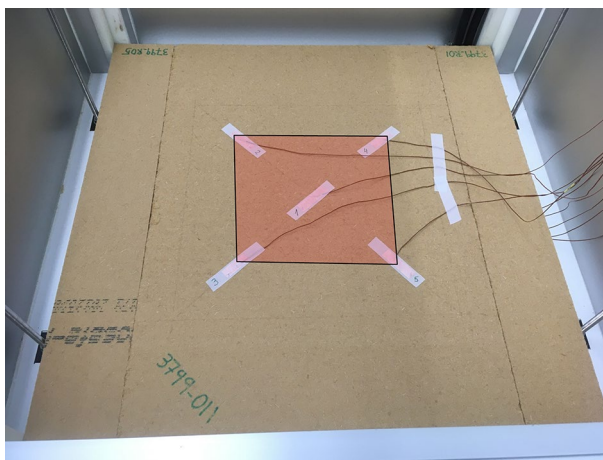

Fig. 4 One of the measured sample halves with the additional temperature sensors (Type K) placed between two identical samples. The surface indicated in light red is the metering area

Fig. 5 Model of the sample configuration used for the numerical analysis including the applied mesh. The yellow part represents the insulation surrounding the samples. The heating and cooling plates were just taken as boundary conditions (Fig. 6). The two samples are represented in light and dark brown (Color figure online)
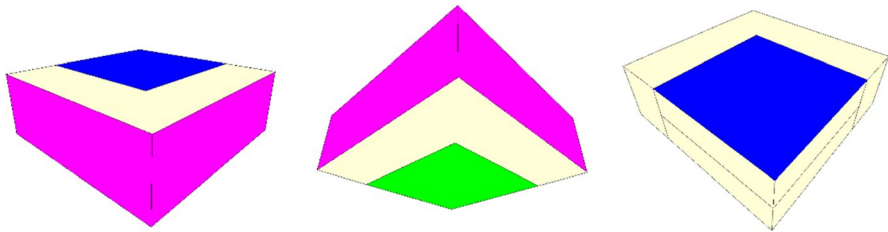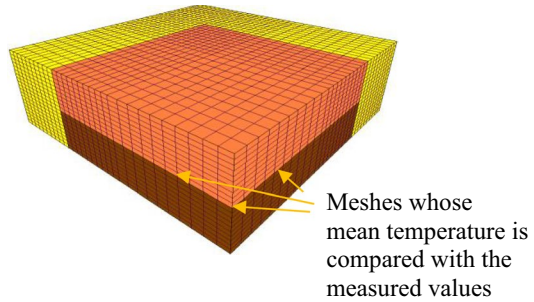

Meshes whose mean temperature is compared with the measured values

Fig. 6 The Boundary conditions applied to surfaces of the model: on the left the top view from the external side, blue representing the hot plate and pink the air in the box of the apparatus in the center the bottom view, green representing the cold plate and pink the air in the box of the apparatus and finally left with a bottom view from the internal side The white parts represent adiabatic boundary conditions (Color figure online)

temperature set point of the heating and the cooling plates (or only one of them) was changed. This started a transient regime and the thermocouples between the two sample halves began to follow the change. At the final step, a new steady state was reached, and the measurement ended then. The temperature evolution between the two sample halves is the quantity that depends on the thermal diffusivity (4) and by inserting the measured values of density and thermal conductivity of each material (Table 1) as input into the numerical simulations, the specific heat capacity can be derived out of it as explained in the following chapter.

4 Numerical Simulations

The aim of the numerical simulations is to reproduce the measured temperatures as accurate as possible where the only unknown input parameter is the specific heat capacity. The evolution of the temperature distribution between the two sample halves, beginning first from a steady state and passing through a transient state and finally ending in another steady state has been calculated by VOLTRA [18] as a comparison to the measured values. To reduce calculation time, the symmetry was exploited by modeling only a quarter of the total sample configuration within the guarded hot plate (Fig. 5). The surfaces and the corresponding boundary conditions applied to them are shown in Fig. 6. These boundary conditions are the measured

temperatures on the warm (Fig. 6 blue), the cold (Fig. 6 green), and in the guarded hot plate apparatus itself (Fig. 6 pink), respectively. Further, there are the adiabatic boundary conditions on top and bottom of the surrounding insulation layer (Fig. 6 white, left, and center) as two temperature boundary conditions cannot intersect in a numerical calculation. These are approximations made to limit the model whose influence is assumed to be limited due to the insulation layer around the samples. There are also those adiabatic boundary conditions (Fig. 6 white, right) which are due to geometrical symmetry to have the smallest representative model to keep time of computation at minimum.

A time step of 30 s, a maximum heat flow divergence for the whole object of 0.001 % and a mesh with 20′181 nodes has been used for all calculations.

5 Results and Discussions

The measured temperatures for two identical wood fiber samples on the warm side, between the two samples and on the cold side, are depicted in Fig. 7. They clearly show that after about 800 min (13 h), a steady state was reached. Then, at about minute 1080 (x-axis), the temperature on the warm side decreases (W1 to W5) because of regulating the heating from 26 °C down to 12 °C. The temperature between the samples follows this decrease (M1 to M5). The cold side (C1 to C5) is kept unchanged at a constant temperature of 5.6 °C. Applying the average measured warm and cold side temperatures as boundary conditions to the simulation, the temperature between the samples is calculated and can be compared to
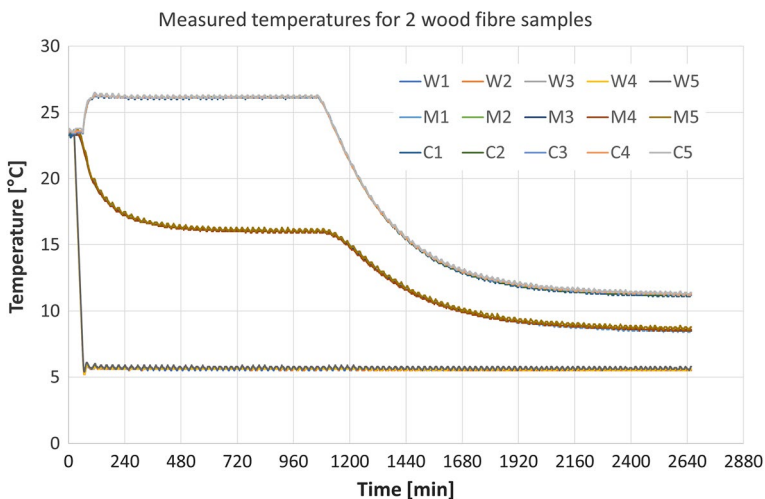

Fig. 7 Measured temperatures on the cold side, in between and on the cold side of 2 wood fiber samples (5 thermocouples each). Standard deviation of the single mean values is around 0.15 K
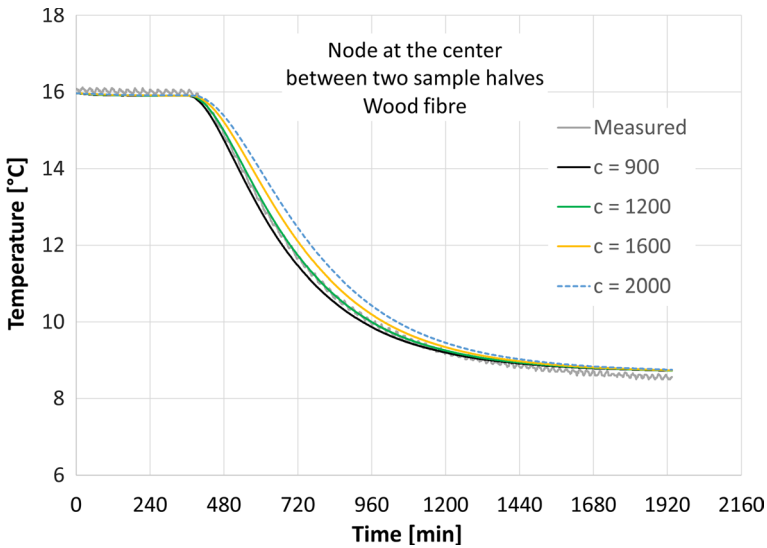
Fig. 8 Measured temperature in wood fiber in comparison to 4 calculated temperatures corresponding to 4 different values assumed for the specific heat capacity

the measured values depending on the value for specific heat capacity as the only unknown (Fig. 8).

A direct comparison between effectively measured temperatures and simulations based on different values assumed for the specific heat capacity is shown in Fig. 8. The value which corresponds best to the measurements for the case of wood fiber is clearly $c = 1200$ J·(kg·K)$^{-1}$. All other curves corresponding to the three other values deviate visibly from the measured curve. The amount of correspondence between measured and calculated values can be improved by more precise values using improved iterative simulation procedures so that an accuracy of ± 10 % can be reached.

A similar procedure with slightly different temperature levels was chosen for the expanded perlite samples. In this case, a steady state was reached where the cold side was stabilized at 10.6 °C (C1 to C5) and the warm side at 21.0 °C (w1 to W5). At the minute 1285 (x-Axis), both temperatures rise due to the regulation of the cold side to reach 20 °C and the warm side to reach 31.0 °C (Fig. 9). The temperatures in between follow this increase in accordance with the thermal properties of the samples. As thickness, density, and thermal conductivity of the samples are known, the only remaining parameter to be identified is the specific heat capacity.

Accordingly, a direct comparison between effectively measured temperatures and simulations based on different values assumed for the specific heat capacity is shown in Fig. 10. The value which corresponds best to the measurements for the case of expanded perlite is $c = 900$ J·(kg·K)$^{-1}$. All other curves corresponding to the three other values deviate visibly from the measured curve. Here too, more
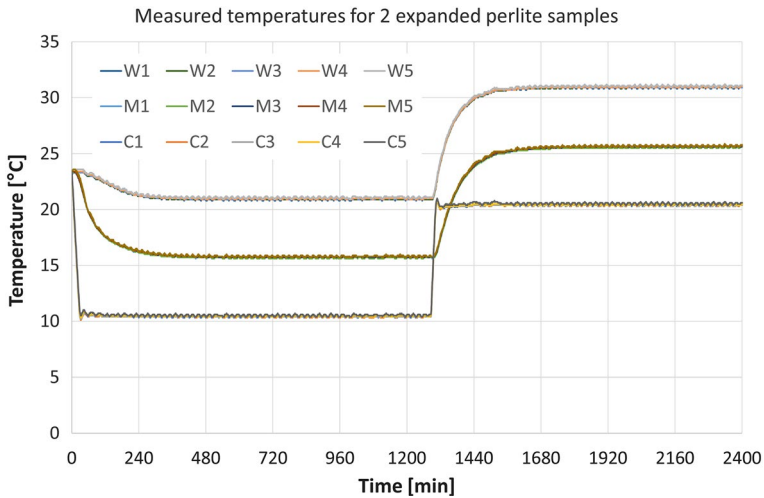
Fig. 9 Measured temperatures on the cold side, in between and on the cold side of 2 expanded perlite samples (5 thermocouples each). Standard deviation of the single mean values is around 0.15 K
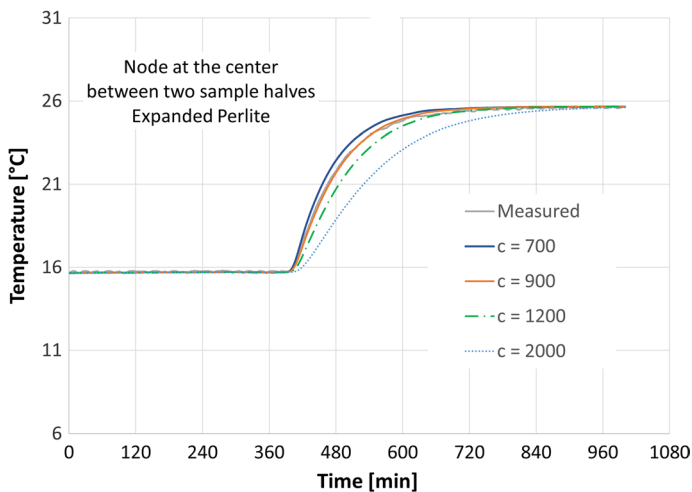

Fig. 10 Measured temperature in expanded perlite in comparison to 4 calculated temperatures corresponding to 4 different values of the specific heat capacity

precise values leading to an of ± 10 % can be reached using improved iterative simulation procedures.

The results clearly show the difference between wood-based and mineral-based materials based on sample sizes representative for porous and fibrous building materials.

The difference in temperature regimes applied to the two materials (Figs. 7 and 9) is to show that there is a variety of possibilities to execute the measurements

within the boundary conditions of the guarded heat plate and get acceptable results. The higher the temperature gap at the starting point is, the higher is the accuracy of the results. But this is limited to the range the guarded hot plate is designed for.

Most producers of building insulation materials supply data sheets which do not include the specific heat capacity of their products and is some of them do, then it is not clear with which method these values were determined. This fact makes it difficult to compare the present results with comparable data. The only way would be to measure the same material with all different methods which would need more elaborate investigations.

6 Conclusions and Outlook

The guarded hot plate apparatus is besides its main use to determine thermal conductivity a useful device to also determine the specific heat capacity of building insulation materials which cannot be done in small calorimeter devices due to the low density, low thermal conductivity, and inhomogeneous structure of the samples. The only additional equipment needed are temperature sensors with a corresponding data acquisition device and a software able to calculate 3-dimensional transient temperature distributions. The accuracy can be improved by choosing a large temperature gradient between the hot and cold plate as an initial condition from where the evolution of the temperature starts. This is recommendable for materials containing only a small amount of moisture, preferably in equilibrium with air of 23 °C and 50 % to 60 % of relative humidity. This is to keep the influence of moisture transport during the transient procedure at a negligible level. The accuracy of the determined specific heat capacity can be improved by applying an iterative procedure minimizing the differences between measurement and calculation. An improved version of this procedure has the potential to become a standard method to determine the specific heat capacity at ambient temperatures for this kind of materials. Investigation is still needed to quantify the influence of approximations made by using adiabatic boundary conditions between the 3 temperature boundary conditions.

Author Contributions K.GW. wrote the main manuscript including figures. K.GW. and W.R. prepared samples, executed the tests. K.GW. evaluated the data. K.GW. and T.R. wrote the internal application. All authors reviewed the manuscript.

Data Availability By contacting the corresponding author.

Declarations

Conflict of interest No conflict of interest to be declared. No external funds were used for this investigation.

Ethical Approval Not applicable.

References

1. K. Nandi, A. Nandi, T. Litchey, Mater. Struct. **45**, 1465 (2012). https://doi.org/10.1617/s11527-012-9850-1
2. M.N. Özişik, *Heat Transfer. A Basic Approach* (McGraw-Hill, Singapore, 1985), pp. 101–105
3. D. Mann, R.E. Field, R. Viskanta, Heat Mass Transf. **27**, 225 (1992). https://doi.org/10.1007/BF01589920
4. A. Bouguerra, A. Aït-Mokhtar, O. Amiri, M.D. Diop, Int. Commun. Heat Mass Transf. **28**, 1065 (2001). https://doi.org/10.1016/S0735-1933(01)00310-4
5. T. Boumaza, J. Redgrove, Int. J. Thermophys. **24**, 501 (2003). https://doi.org/10.1023/A:1022928206859
6. T. Ohmura, M. Tsuboi, M. Onodera, T. Tomimura, Int. J. Thermophys. **24**, 559 (2003). https://doi.org/10.1023/A:1022936408676
7. S.Y. Zhao, B.M. Zhang, S.Y. Du, Int. J. Thermophys. **30**, 2021 (2009). https://doi.org/10.1007/s10765-009-0680-5
8. H. Park, M. Ruellan, A. Bouvet, E. Monmasson, R. Bennacer, *11th International Conference on Electrical Power Quality and Utilisation*, Oct 17–Oct 19, 2011, Lisbon, Portugal https://doi.org/10.1109/EPQU.2011.6128822
9. H. Park, N. Martaj, M. Ruellan, R. Bennacer, E. Monmasson, J. Electr. Eng. Technol. **8**, 742 (2013). https://doi.org/10.5370/JEET.2013.8.5.742
10. C. Luo, B. Moghtaderi, S. Hands, A. Page, Energy Build. **43**, 379 (2011). https://doi.org/10.1016/j.enbuild.2010.09.030
11. C. Barreneche, A. de Gracia, S. Serrano, M.E. Navarro, A.M. Borreguero et al., Appl. Energy **109**, 421 (2013). https://doi.org/10.1016/j.apenergy.2013.02.061
12. Ł Czajkowski, W. Olek, J. Weres, R. Guzenda, Wood Sci. Technol. **50**, 537 (2016). https://doi.org/10.1007/s00226-016-0803-7
13. F. Barreca, G. Modica, S. Di Fazio, V. Tirella, R. Tripodi, C.R. Fichera, J. Agric. Eng. **XLVIII**, 203 (2017). https://doi.org/10.4081/jae.2017.677
14. R. Ricciu, L.A. Besalducha, A. Galatioto, G. Ciulla, Renew. Sustain. Energy Rev. **82**, 1765 (2018). https://doi.org/10.1016/j.rser.2017.06.057
15. Lakatos, A. Csík, I. Csarnovics, Case Stud. Therm. Eng. **25**, 100966 (2021). https://doi.org/10.1016/j.csite.2021.100966
16. K. Ghazi Wakili, B. Binder, R. Vonbank, Energy Build. **35**, 413 (2003). https://doi.org/10.1016/S0378-7788(02)00112-3
17. EN 12667, Thermal performance of building materials and products—determination of thermal resistance by means of guarded hot plate and heat flow meter methods—products of high and medium thermal resistance. CEN/CENELEC, Brussels, Belgium (2001)
18. VOLTRA Transient thermal simulation of 3D rectangular shapes, Physibel, Gent, Belgium https://www.physibel.be/en/products/voltra

Publisher's Note Springer Nature remains neutral with regard to jurisdictional claims in published maps and institutional affiliations.